INNSPUB

Journal of Biodiversity and Environmental Sciences (JBES)
ISSN: 2220-6663 (Print) 2222-3045 (Online)
Vol. 24, No. 6, p. 91-102, 2024
http://www.innspub.net

RESEARCH PAPER OPEN ACCESS

Green synthesis and characterization of silver and copper bimetallic nanoparticles: Investigation of their biological and photocatalytic potential for the photocatalytic degradation of dye

T. Madhumitha[1], M. Margret Leema[2], E. Amutha[1], E. Pushpalakshmi[1], M. Earnest Stephen Gnanadoss[4], S. Rajaduraipandian[3], G. Annadurai[*1]

[1]*Sri Paramakalyani Centre of Excellence in Environmental Sciences, Manonmaniam Sundaranar University, Alwarkurichi, India*

[2]*Department of Chemistry, Arignar Anna College, Manonmaniam Sundaranar University, Aralvoimozhi, India*

[3]*Sri Paramakalyani College, Manonmaniam Sundaranar University, Alwarkurichi, India*

[4]*Department of Physics, Sri Venkateswara College of Engineering and Technology, Chittoor, Andra Pradesh, India*

Article published on June 11, 2024

Key words: Green synthesis, Bimetallic nanoparticles, Antibacterial activity, Rhodamine dye, Photocatalytic degradation

Abstract

In materials science, green synthesis has gained extensive attention as a reliable, sustainable, and eco-friendly protocol for synthesizing a variety of materials and nanomaterials, such as metal/metal oxide nanoparticles, hybrid materials, and bioinspired materials. As such, green synthesis is regarded as an important tool to reduce the destructive effects associated with the traditional methods of synthesis for nanoparticles commonly utilized in laboratory and industry. They are environmentally friendly because the toxic chemicals produced during the biosynthesis of the nanoparticles can be degraded with the help of enzymes present in the microbes. In this study, we compiled the basic procedures and workings of green synthesis methods, particularly as they relate to the bimetallic synthesis of Ag and Cu nanoparticles utilizing natural extracts. FT-IR, XRD, PSA, FL, and TGA were used to characterize the synthesized Ag-Cu nanoparticles. In addition, silver nanoparticles were used as a potential photocatalyst for the effective degradation of Rhodamine dye under UV light illumination, achieving an efficiency of roughly 84 % after 180 minutes. The antibacterial activity was tested on *B. subtilis, E. coli, Staphylococcus, Enterobacter and Pseudomonas*. Physicochemical properties increased the antibacterial activity of Cu/Ag NPs by causing a homogenous distribution and reducing oxidation and agglomeration. The work's findings demonstrate the advantages of employing a geometrical substrate to increase the antibacterial activity of bimetallic nanoparticles (NPs). This could potentially lower the need for pure Cu/Ag salts in NP-based antibacterial applications.

***Corresponding Author:** G. Annadurai ✉ gannadurai@msuniv.ac.in

Introduction

The multidisciplinary field of nanoscience includes materials science, chemistry, physics, and medicine. As nanotechnology develops, it will significantly influence nearly every aspect of business and society, gaining it the nickname "general-purpose technology" (Singh *et al.*, 2019). "Nanotechnology" was coined by Norio Taniguchi of Tokyo University of Science. According to Sharma *et al.* (2009 & 2019), the Greek word "dwarf," from which the prefix "Nano" is derived, refers to objects that are one-billionth the size of an actual object. Nanotechnology, as defined by Mortazavi *et al.* (2017), is the study of molecules and structures in the 1-100 nm nanometer range. Nanotechnology is one type of technology that is employed in practical applications like electronics. NPs are divided into a wide range of groupings based on their morphological, chemical, and physical characteristics. These include metal NPs, carbon NPs, lipid-based NPs, ceramic NPs, polymeric NPs, and semiconductor NPs. Different features distinguish metal nanoparticles (NPs) from their bulk counterparts. These factors, which improve molecule interaction, include a high surface-to-volume ratio and a degraded density of energy state (Maghsoodi *et al.*, 2019). Biological resources such as plant extract and microorganisms such as bacteria, algae, fungus, viruses, and yeast are used as reducing agents in the green synthesis process. Microorganisms utilized in biosynthesis require aseptic conditions and culture media to develop (Kalishwaralal *et al.*, 2010). Plant extract is considered to be more advantageous than microorganisms since it is easily produced and widely available (Riaz *et al.*, 2020). Plants are extremely predisposed to create them since they are renewable, biodegradable, easy to handle, and rapidly provide natural stabilizing agent to nanoparticles (NPs) (Shankar *et al.*, 2004). Alkaloids, flavonoids, proteins, polyphenols, amino acids, reducing sugars, enzymes, and a variety of other bioactive compounds found in plant extracts may be involved in the bio-reduction of metal ions to metal NPs as well as the stabilization or capping of metallic NPs. The green synthesis of nanoparticles (NPs), which have a wide range of applications in fields like powder metallurgy, magnetic devices, photocatalysis, microelectronic devices, anticorrosive coatings, and biomedical fields, is affected by the parts of the plant, the extraction solvent, the pH of the solution, the concentration of salt, and the reaction temperature (Salem and Fouda, 2021). Ag-Cu nanoparticles were becoming a more significant substance in this new era because of their wide range of biological, dental, and electronic device uses. Because of their exceptional electrical and thermal properties, which have led to a high demand for them in the market, Ag and Cu nanoparticles offer significant promise in a wide range of applications. While silver nanoparticles have proven to be the most effective due to their good antimicrobial agent against bacteria, viruses, and other eukaryotic microorganisms, Ag nanoparticles have drawn a lot of attention due to their excellent broad-spectrum antimicrobial activity (Rai *et al.*, 2009; Tran *et al.*, 2013; Hikmah *et al.*, 2016). Carroll *et al.* (2011) reported that antibacterial activity of metal nanoparticles like Ag and Cu was discovered. Because of their small size and high surface to volume ratio, which enable them to interact closely with microbial membranes, metal nanoparticles have been shown to have bactericidal effects. This effect is not limited to the release of metal ions in solutions. The metal nanoparticles' antibacterial qualities find use in a variety of industries, including water treatment, food processing, medical equipment, and gadgets (Rai *et al.*, 2009; Hikmah *et al.*, 2016). According to Yoon *et al.* (2007) heavy metal removal and microbe inactivation are two of the features of silver and copper nanoparticles. By applying the nano antimicrobial metals to the surfaces of medical equipment and water treatment filters that need to have antimicrobial properties, they can be employed efficiently (Yoon *et al.*, 2007; Hikmah *et al.*, 2016). Numerous plant extracts, including *Azadirachta indica* (neem), *Aloe vera*, *Emblica Ofcinalis* (amla), and *Cinnamomum camphora*, have already been shown to form silver nanoparticles (Canizal *et al.*, 2001; Shankar *et al.*, 2004; Ankamwar *et al.*, 2005; Krishnaraj *et al.*, 2005; Chandran *et al.*, 2006; Alok KumarGiri *et al.*, 2022). Unfortunately, there is no information available regarding the synthesis of silver

nanoparticles from the plant *Eugenia roxburghii*, nor about any of their biological applications. Therefore, an attempt was undertaken to create silver nanoparticles from the leaf extract and investigate their antimicrobial properties in this work. The primary goal of this research project is to use the extract from *Lantana camara* leaves to create bimetallic copper-silver nanoparticles. XRD, SEM, EDX, and particle size analyzer analyses were used to evaluate the produced bimetallic nanoparticles. The antibacterial properties of the nanoparticles against Gram-positive and Gram-negative bacterial strains were confirmed, as was their catalytic activity in the breakdown of Rhodamine dye from aqueous solution.

Materials and methods

Chemicals and plant material collection

All the reagents purchased were of analytical grade and used without any further purification. Silver nitrate ($AgNO_3$) and Copper nitrate ($CuNO_3$) was purchased from Sigma-Aldrich with ≥ 99.5% purity. Fresh leaves of *Lantana camara* were collected from the local area land, Idaikal, India. Distilled water was used for preparing aqueous solutions all over the experiments.

Preparation of leaf extract

Aqueous leaves extracts were prepared by the following procedure:

Fresh leaves of *Lantana camara* were collected and washed with tap water at first, and then the surface was washed under running water with distilled water until no impurities remained. Then, the fresh leaves were cut and weighed about 10g and dissolved in 100 mL of distilled water. The mixture was heated for 20 minutes at 60°C while stirring occasionally and then allowed to cool at room temperature. The mixture was filtered using the Whatman no: 1 filter paper. The extract was stored in the refrigerator for further use to synthesize Ag-Cu nanoparticles from the $CuNO_3$, $AgNO_3$ precursor solution.

Green synthesis of Ag-Cu bimetallic nanoparticles

$AgNO_3$ powder was dissolved in distilled water to prepare a 200 mL stock solution in a flask and maintained in magnetic stirrer for 20 minutes. $CuNO_3$ powder was dissolved in distilled water to prepare a 200 mL stock solution in a flask and maintained in magnetic stirrer for 20 minutes. Both the metal salt solutions were mixed and heated for 10 min at 95 °C. 40 mL of the plant extract was added to the salt solution. The mixture was maintained at room temperature for 24 h followed by centrifugation, and dried at Hot air over at 60°C for 24 h.

Photocatalytic activity

We synthesized 20 ppm Rhodamine dye in 100 mL deionized water to test the photocatalytic activity of biogenic Ag-Cu NPs. The original concentration (5 mL) was removed from the solution, and 100 mg (0.1 g) of Ag-Cu NPs catalyst was added to 100 mL of dye solution; the solution was kept in the dark for 20 minutes to maintain the adsorption desorption equilibrium, then exposed to UV light, and samples were taken at various time intervals. To remove the catalyst from the samples, centrifugation at 5000 rpm for 15 minutes was used; the degradation of dye was measured using a UV visible spectrophotometer. The following formula was used to compute the % degradation of the deteriorated dye:

$$\text{Degradation efficiency (\%)} = CI\text{-}CF/CI\times100 \quad (1)$$

Where CI = initial Rhodamine dye concentration (g/L), and CF = concentration of the Rhodamine dye solution after the degradation time.

Antibacterial activity

The antibacterial activity of the fabricated Ag-Cu NPs was tested against five bacterial species, including *Escherichia coli*, *Staphylococcus aureus*, *Bacillus subtilis*, *Enterobacter*, and *Pseudomonas fluorescens*, using the well-diffusion method. The bacterial strains were cultured in nutrient broth for around 24 hours at 37 °C. 100 mL of muller hinton agar was poured into Petridishes and incubated. 20 mL of muller hinton agar was put into the Petridishes and allowed to cool. All of the bacteria suspensions were switched over the medium and the wells were filled at four different concentrations of nanoparticle solution: 25,

50, 75, and 100 µL. The plates were incubated for 24 hours at 37 °C. Three different orientations were used to measure the inhibition zone that formed around each well. The zones of inhibition of the examined microorganisms by the compounds were measured on a millimeter scale.

Results and discussion

UV visible spectroscopy analysis

Ag-Cu NPs' optical characteristics were assessed by measuring their UV–vis spectra (Fig.1). Ag-Cu NPs' absorption spectra shows a characteristic Ag surface plasmon resonance (SPR) band, which peaks at approximately 310 nm and spans 200 to 380 nm. The brown color of the solution indicates that the biomolecule-covered synthetic silver and copper nanoparticles are evenly distributed throughout the solutions and are reasonably stable for up to three months. These findings unambiguously show that, in the case of copper nanoparticles, a mixture of CuO and Cu_2O nanoparticles formed, as previously documented in the literature (Rickerby *et al.,* 2007; Saada *et al.,* 2021).

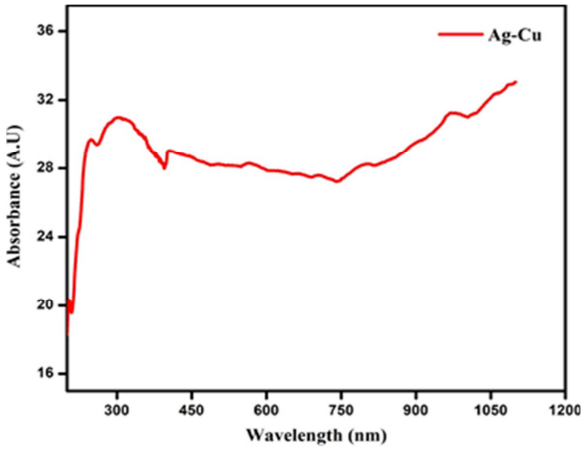

Fig. 1. UV spectrum of Ag-Cu NPs

Fourier transform infrared spectroscopy analysis

The wave number range for FTIR analysis is 450/cm to 4000/cm. Prior to FTIR analysis, the material was combined with KBr, well mixed, and pelletized by crushing it under enough pressure. Ag-Cu NPs are examined using an FTIR spectrophotometer and displayed in Fig. 2. The peak was measured at 3441 cm^{-1} for phenols, O-H stretch, and H-bonded alcohols (Table 1).

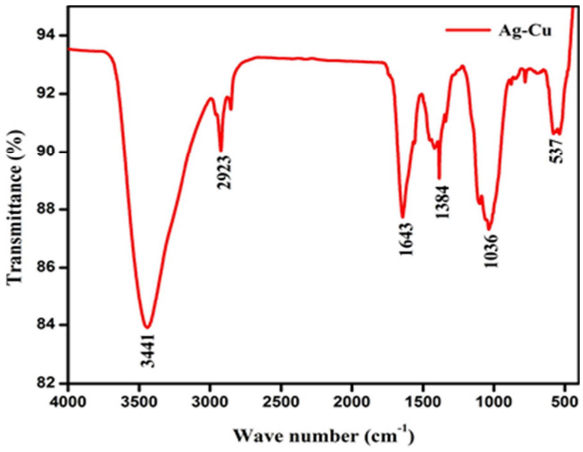

Fig. 2. FT-IR spectra of Ag-CuNPs

Table 1. Peak table of Ag-Cu NPs

S.No	Peak (cm^{-1})	Functional group
1	3441	O–H stretch, H–bonded alcohols, phenols
2	2923	C–H stretch alkanes
3	1643	C=C stretch (conjugated) alkenes
4	1384	C-F stretch alkyl halides
5	1036	C-N Amines
6	537	C–Br stretch alkyl halides

C–H stretch alkanes are linked to the peaks at 2923 cm-1 (Therese Marie and Drexel, 2016; Hikmah *et al.*, 2016). The peak at 2025 cm-1 is connected to the C=N stretch of nitrile. Alkenes that were conjugated with a C=C stretch were linked to the peak at 1643 cm-1. C-N Amines are linked to the peaks at 1036 cm-1. For C–Br stretch alkyl halides, 1384 cm–1 was the peak obtained. The peaks showed that the *Lantana camara* aqueous extract included several functional groups that were responsible for the production of stable Ag-CuNPs (Wang *et al.,* 2021; Sujitha and Kannan, 2013).

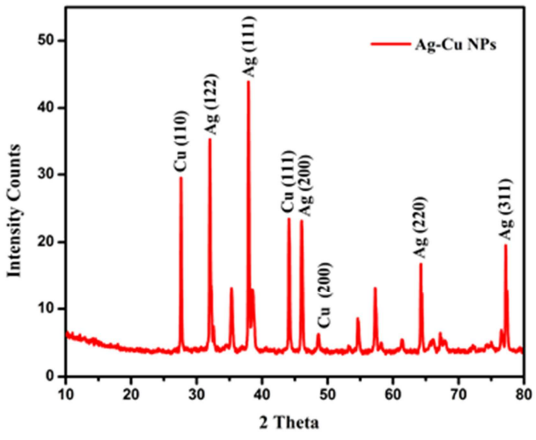

Fig. 3. XRD pattern of Ag-CuNPs

X-ray diffraction analysis

XRD analysis is used to study the phase and crystal structure of the produced nanoparticles. Fig. 3 displays the Ag-Cu nanoparticles XRD patterns. According to Khot *et al.* (2001), the principal distinctive diffraction peaks for silver are detected at 27.6, 46.06, 54.65, 67.30, and 77.19. These peaks correspond to the crystallographic planes of (110), (111), (211), (222), and (311), respectively. Three significant distinctive diffraction peaks for copper have been observed: 32.0 and 74.29, which match the crystallographic planes of (220) and (111). The findings align with those of Jayaseelana *et al.* (2012), wherein all eight distinctive diffraction peaks of copper and silver were observed (Nidhi and Agrawal, 2021).

The face centered cubic (fcc) phases of crystalline Ag (JCPDS card no. 4-783) and crystalline Cu (JCPDS card no. 4-836) are well indexed to all of the peaks. The bimetallic NP peaks lie between the Ag and Cu peaks, suggesting that the newly produced phases are homogenous Ag-Cu alloy phases rather than Ag and Cu phases that are totally separated. As per Bosetti *et al.* (2002) and Benassai *et al.* (2021), the creation of alloy nanoparticles is also indicated by the variation in lattice parameter. In all known highly reactive samples, the silver nanoparticles have a high atomic density facet of (111) (Hikmah *et al.*, 2016). Ag-Cu bimetallic nanoparticles have an average crystallographic size of 24 nm.

Dynamic light scattering analysis

After being ultrasonically sonicated, the produced Ag-Cu NPs were suspended in the ethanol solution. Using a particle size analyzer, the diameters of the agglomerated colloids in the suspensions were calculated.

According to the analysis, the particle size is 60 nm, which is twice the Ag-Cu NPs crystallite size and in good agreement with the crystallite size (Araya Castro *et al.*, 2020).

Fig. 4 displays the Ag-CuNPs particle size distribution and average particle size data. However, since the bimetallic nanoparticles differ in many ways—including dispersion color, surface plasmon resonance (UV), shape or morphology (SEM), among others—the development of a physical combination in either sample can be ruled out. It is known that the synthetic method utilized to generate bimetallic nanoparticles affects the distribution and arrangement of each metal within a particle (Allan *et al.*, 2015). When using DLS, light is directed toward a suspension of particles from a coherent source and dispersed there (Ajitha *et al.*, 2015; Ahmed *et al.*, 2016). The scattering varies throughout time as a result of the scatterers ever-changing distances from one another, which is caused by the particles' unpredictable Brownian motion. Therefore, when palladium is taken into account, the size of the ionic liquid and plant extract mediated nanoparticles, as assessed by DLS, may look smaller than the plant mediated nanoparticle without ionic liquid. In the majority of investigations, plant-mediated nanoparticles quickly aggregate. In this work, DLS is recorded after aging for four hours. Previously, the size distribution profile of nanoparticles in suspension was established using DLS.

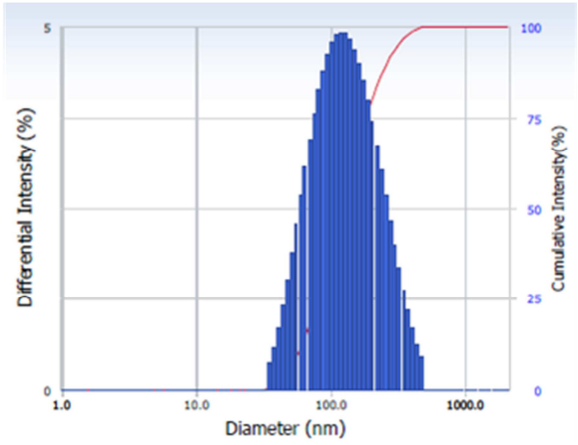

Fig. 4. DLS image of Ag-CuNPs

Scanning electron microscopy (SEM) and EDAX

Fig.5 displays the Ag-Cu NPs' SEM pictures. The structural and morphological behavior of the bimetallic nanoparticles is supported by the SEM pictures. It is evident that when plant extract was employed as a capping and reducing agent, Ag-Cu NPs of various forms were produced. Ag-Cu NPs

produced nanostructures with roughly spherical agglomerated and indefinable forms, respectively. This could be because the various nanoparticles contain varying amounts and types of capping agents. The FTIR analysis's findings about the shifts and differences in areas of the peaks corroborate this (Devatha *et al.,* 2018a; 2018b). SEM and EDS examination In addition to studying the Ag-Cu core-shell nanoparticles' surface morphology, the SEM micrographs are used to corroborate the XRD result. The enhanced SEM micrograph of Ag-Cu nanoparticles at various molarities is displayed in Fig. 5. Fig. 5 illustrates how comparable the surface morphology and roughness are for the two samples. The particles have a narrow size distribution and are uniformly distributed in nanoscale size. The majority of particles have a spherical form (El-Adawy *et al.,* 2020; Elango and Roopan, 2015). Fig. 5 illustrates how the surface agglomerates and is rough. It is extremely challenging to distinguish between the different particles. It results from an incomplete reduction process between the reactants, which produces Cu particles. As previously mentioned, the reduction reaction became incomplete due to the high concentration of Cu in solutions. The results show good agreement with the XRD findings.

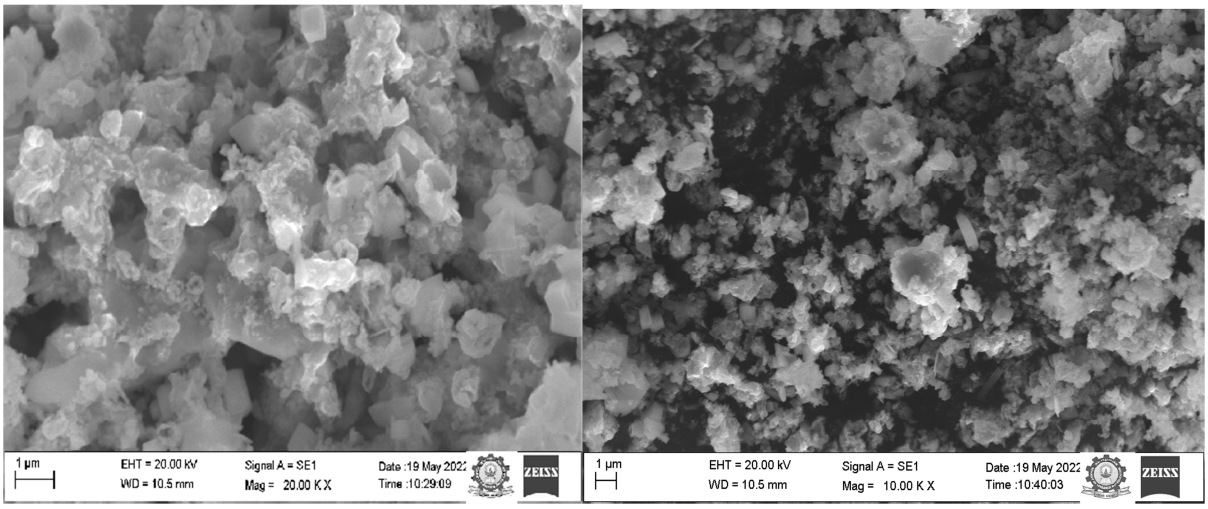

Fig. 5. SEM image of Ag-Cu NPs

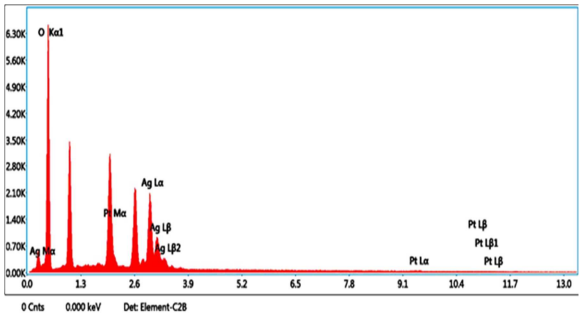

Fig. 6. EDAX spectrum of Ag-Cu NPs

To comprehend the semi-quantitative elemental composition of Ag-Cu NPs, EDX analysis was performed. Particles of copper and silver were visible in the peaks (Fig. 6). In order to support the purity of metallic nanoparticles, the total metal content was rather high (Gao *et al.,* 2018).

Fluorescence spectroscopy analysis

Ag-CuNPs' room temperature fluorescence spectra were captured using a fluorescence spectrophotometer, as depicted in Fig.7. 400–900 nm was the wavelength range over which measurements were taken. The trials yielded maximum wavelength emission intensities, as illustrated in Fig. 7. The emission data were then plotted as wavelength (nm) vs. intensity (A.U.). As was previously said, the degree of aggregation and particle size are significantly influenced by the spinning electrode's rotation speed, with smaller nanoparticle formation being more advantageous at higher rotational speeds.

Additionally, we noticed that the size of the generated Ag-Cu NPs decreased in tandem with an increase in the rotating electrode's rotation speed (Guo *et al.,* 2021). Ag-Cu NPs have three distinct peaks, as seen in Fig. 7.

A greater emission peak was recorded with an excitation wavelength of 804 nm, which may have been caused by surface imperfections. The lower emission peak was assigned at 441 nm, signifying the Ag-CuNPs production. The best method for examining energy levels was to use fluorescence spectra. There was a noticeable rise in fluorescence intensity when Ag-Cu NP size increased.

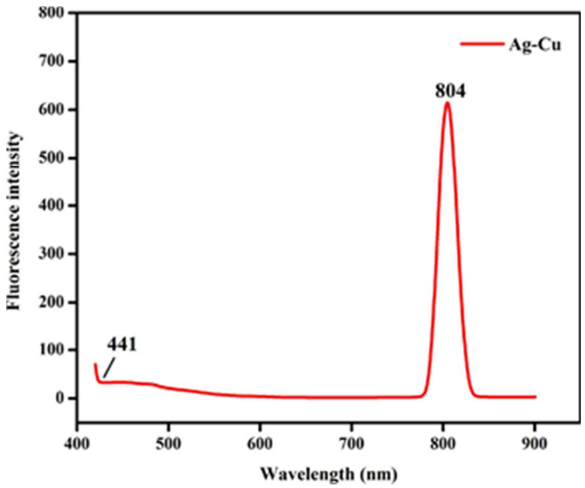

Fig.7. Fluorescence spectrum of Ag-Cu NPs

Fig. 8. Zone of inhibition of Ag-Cu NPs against various bacterial strains

Antibacterial activity

Using the agar well diffusion method, the antibacterial activity of integrated Ag-Cu NPs was tested against *Staphylococcus aureus*, *Bacillus subtilis*, *Enterobacter* sp., *Pseudomonas auroginosa*, and *E. coli* (Fig. 8). Using sterilized cotton swabs, a 24-hour culture of pathogenic bacteria strains was evenly swabbed onto each person's plates containing Muller hinton agar. Pathogenic bacteria are cultivated in nutritional broth. Five or so wells were created, and each well on all plates received varying weights of pure Ag-Cu NPs—25, 50, 75, and 100 µl. In an incubator, the plates were incubated for twenty-four hours at 37°C. Following incubation, measurements were made of the various zones that formed around the well (Gopinath *et al.*, 2014). Additionally, compared to Ag nanoparticles, Cu nanoparticles' zone of inhibition is slightly larger. The zone of inhibition in bimetallic systems rises as Cu concentrations do, so bolstering the effectiveness of Cu nanoparticles once more. Even at concentrations as low as 0.3 mg/L, the metallic nanoparticles had good antibacterial efficacy against bacteria, according to the data. Therefore, given the stable dispersion at the molecular level in the solution, it is possible to conclude that copper and silver ions may be released through aqueous starch solutions. The antibacterial activity is caused by the gradual migration of metal ions from the stabilizing medium. One could reasonably assume that the combination of metallic nanoparticles with biopolymers will prolong the Ag particle's release period and maintain its prolonged antibacterial activity (Jabir *et al.*, 2021; Kargara *et al.*, 2015).

Table 2. Zone of inhibition of Ag-Cu bimetallic NPs against selected bacterial strains

	Zone of inhibition (mm in diameter)				
Concentration	*Bacillus*sp.	*E. coli*	*Enterobacter* sp.	*Staphylococuus aureus*	*Pseudomonas* sp.
25 µl	1.2	1.2	1.6	1.5	1.1
50 µl	1.2	1.4	1.7	1.7	1.2
75 µl	1.4	1.7	2.0	1.9	1.4
100 µl	1.6	1.9	2.1	2.0	1.6

Additionally, Table 2 data show that the nanoparticles work better against *E. coli* than *S. aureus*. According to (Kilkarni and Muddapur, 2014; Kumar Panda *et al.*, 2021), Gram-negative and Gram-positive microbes differ in their cell wall structure, which accounts for the higher biocidal effectiveness of silver nanoparticles against *E. coli*. Contrary to previous reports (Ma *et al.,* 2021; Mehwish *et al.,* 2021), which attributed the decreased activity of copper nanoparticles to the oxide layer present on the surface, copper was shown to be more efficient than silver among the two metals (Naseer *et al.,* 2021).

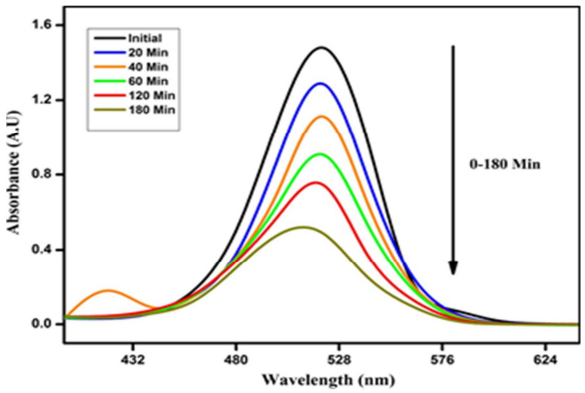

Fig. 9. UV–visible spectra of Rhodamine dye degradation with Ag-Cu NPs

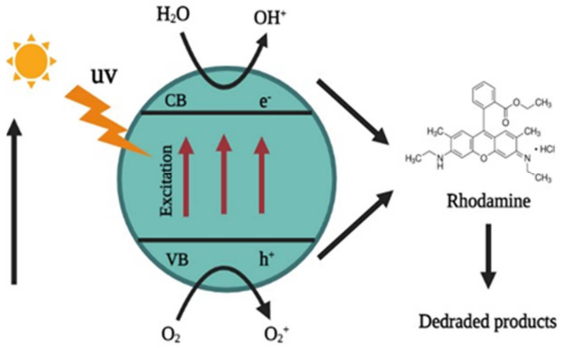

Fig. 10. Reaction Mechanism for the Degradation of Rhodamine

Photocatalytic activities of Ag-Cu NPs for the degradation of rhodamine dye

Effect of irradiation time

Fig. 9 illustrates how the degradation of dye grew with increasing UV light irradiation during the first 20 minutes, peaking at 88% after 180 minutes. As the time interval rose, so did the dye's degradation (Singh *et al.*, 2018).

Mechanism of photocatalytic catalytic degradation of the dye

We've already examined the connection between deterioration and time; the next step is to determine how this degradation takes place. Researchers examined how time affected the deteriorating process in order to determine the mechanism (Dhandapani *et al.,* 2012). Fig. 10 illustrates how the breakdown of rhodamine dye is a light-dependent process.

In order to enable valence electrons to move from the valence band to the conduction band, the dye must first be adsorbed on the surface of the catalyst, in this case Ag-Cu NPs. During this process, a positive hole, h+, is lifted inside the valence band. Adsorbed water molecules on the surface of the photocatalyst will combine with the positive holes and free electrons to form ·OH radicals, while the free electrons will change the dissolved oxygen into superoxide anion O_2· radicals. These light-generated radicals break down the dye molecules into simpler molecules like CO_2 and H_2O.

Ag-Cu NPs + hν → e^- + h^+

$H_2O + h^+ \rightarrow OH\cdot + H^+$

$O_2 + e^- \rightarrow O2\cdot -$

OH + dye → degradable product

$O_2^- +$ dye → degradable product

Conclusion

The green production of bimetallic Ag-Cu NPs using leaf extract from *Lantana camara* is highlighted in this work. The use of *Lantana camara* leaf extract as a capping reagent to lower the average bimetallic particle size to 80 nm was innovative to this work. Numerous structural and morphological analyses of the nanoparticles as they were created using UV, FTIR, particle size analyzer, SEM, EDX, and XRD revealed that copper–silver nanoparticles were fully synthesized with very little of their respective oxides. Application investigations for the as-prepared bimetallic nanoparticles demonstrated their strong antibacterial activity, demonstrating that the zones of inhibition for Gram-positive and Gram-negative bacteria were almost identical. Under UV light, Ag-Cu

nanoparticles demonstrated noticeable photocatalytic activity against Rhodamine dye, with an estimated 92% destruction efficiency in 240 minutes. Thus, a low-cost, non-toxic, environmentally friendly method for creating superior copper-silver bimetallic nanoparticle system is reported. As a potential extension of the current work, a thorough investigation into the industrial and commercial use of the produced bimetallic nanoparticles may be conducted.

References

Ahmed S, Ahmad M, Swami BL, Ikra S. 2016. A review on plants extract mediated synthesis of silver nanoparticles for antimicrobial applications: A green expertise. Journal of Advanced Research **7,** 17-28.

Ajitha B, Ashok Kumar Reddy Y, Sreedhara Reddy P. 2015. Green synthesis and characterization of silver nanoparticles using *Lantana camara* leaf extract. Materials Science and Engineering: C **49,** 373–381.

Allan J, Belz S, Hoeveler A, Hugas M, Okuda H, Patri A, Rauscher H, Silva P, Slikker W, Sokull-Kluettgen B, Tong W, Anklam E. 2021. Regulatory landscape of nanotechnology and Nano plastics from a global perspective. Regulatory Toxicology and Pharmacology **122,** 104885.

Alok Kumar G, Biswajit J, Bhagyashree B, Arun Kumar P, Manoranjan A, Saumyaprava A, Laxmikanta A. 2022. Green synthesis and characterization of silver nanoparticles using *Eugenia roxburghii* DC. extract and activity against biofilm producing bacteria. Scientific Reports **12,** 8383.

Ankamwar B, Damle C, Ahmad A, Sastry M. 2005. Biosynthesis of gold and silver nanoparticles using *Emblica officinalis* fruit extract, their phase transfer and transmetallation in an organic solution. J. Nanosci. Nanotechnol **5,** 1665–1671.

Araya-Castro K, Chao TC, Duran-Vinet B, Cisternas C, Ciudad G, Rubilar O. 2020. Green synthesis of copper oxide nanoparticles using protein fractions from an aqueous extract of brown algae *Macrocystis pyrifera*. Processes **9(1),** 1-10.

Benassai E, Del Bubba M, Ancillotti C, Colzi I, Gonnelli C, Calisi N, Salvatici MC, Casalone E, Ristori S. 2021. Green and cost-effective synthesis of copper nanoparticles by extracts of non-edible and waste plant materials from *Vaccinium* species: characterization and antimicrobial activity. Materials Science and Engineering: C **119,** 111453.

Bosetti M, Masse A, Tobin E, Cannas M. 2002. Silver coated materials for external fixation devices: in vitro biocompatibility and genotoxicity. Biomaterials **23,** 887-892.

Canizal G, Ascencio JA, Gardea-Torresday J, Jose-Yacamán M. 2001. Multiple twinned gold nanorods grown by bio-reduction techniques. J. Nanopart. Res **3,** 475–48.

Carroll KJ, Reveles JU, Shultz MD, Khanna SN, Carpenter EE. 2011. Synthesis and characterization of silver-copper core-shell nanoparticles using polyol method for antimicrobial agent. J. Phys. Chem. C **115,** 2656–2664.

Chandran SP, Chaudhary M, Pasricha R, Ahmad A, Sastry M. 2006. Synthesis of gold nanotriangles and silver nanoparticles using *Aloe vera* plant extract. Biotechnol. Prog **22,** 577–583.

Devatha CP, Thalla AK. 2018a. Green synthesis of nanomaterials. Synthesis of Inorganic Nanomaterials, 169–184.

Devatha CP, Thalla AK. 2018b. Chapter 7 - Green synthesis of nanomaterials (S. Mohan Bhagyaraj, O. S. Oluwafemi, N. Kalarikkal, & S. Thomas, Eds.). Science Direct; Woodhead Publishing.

Dhandapani P, Maruthamuthu S, Rajagopal G. 2012. Bio-mediated synthesis of TiO2 nanoparticles and its photocatalytic effect on aquatic biofilm. J Photochem Photobiol B **110,** 43–49.

El-Adawy MM, Eissa AE, Shaalan M, Ahmed AA, Younis NA, Ismail MM, Abdelsalam M. 2020. Green synthesis and physical properties of Gum Arabic-silver nanoparticles and its antibacterial efficacy against fish bacterial pathogens. Aquaculture Research **52(3),** 1247–1254.

Elango G, Roopan SM. 2015. Green synthesis, spectroscopic investigation and photocatalytic activity of lead nanoparticles. Spectrochim Acta Part A **139,** 367–373.

Firdaus ML, Apriyoanda H, Elvinawati E, Rahmidar L, Astuti AP, Swistoro E, Sundaryono A. 2021. Green route of silver nanoparticles synthesis using watermelon (*Citrullus lanatus*) fruit extract for mercury ions detection. Journal of Physics: Conference Series **1731,** 012020.

Gao M, Ye R, Shen W, Xu B. 2018. Copper nitrate: a privileged reagent for organic synthesis. Organic & Biomolecular Chemistry **16(15),** 2602–2618.

Gopinath K, Shanmugam VK, Gowri S, Senthilkumar V, Kumaresan S, Arumugam A. 2014. Antibacterial activity of ruthenium nanoparticles synthesized using *Gloriosa superba* L. leaf extract. J Nanostruct Chem **4,** 83.

Guo X, Mahmud S, Zhang X, Yu N, Faridul Hasan KM. 2021. One-pot green synthesis of Ag@AgCl nanoparticles with excellent photocatalytic performance. Surface Innovations **9(5),** 227-284.

Hikmah N, Idrus NF, Jai J, Hadi A. 2016. Synthesis and characterization of silver-copper core-shell nanoparticles using polyol method for antimicrobial agent. Earth and Environmental Science **36,** 012050.

Jabir MS, Saleh YM, Sulaiman GM, Yaseen NY, Sahib UI, Dewir YH, Alwahibi MS, Soliman DA. 2021. Green synthesis of silver nanoparticles using *Annona muricata* extract as an inducer of apoptosis in cancer cells and inhibitor for NLRP3 inflammasome via enhanced autophagy. Nanomaterials **11(2),** 384.

Jayaseelana C, Rahumana AA, Kirthi AV, Marimuthua S, Santhoshkumara T, Bagavana A. 2012. Novel microbial route to synthesize ZnO nanoparticles using *Aeromonas hydrophila* and their activity against pathogenic bacteria and fungi. Spectrochimica Acta Part A **90,** 78–84.

Kalishwaralal K, Deepak V, Ram Kumar Pandian S, Kottaisamy M, BarathmaniKanth S. 2010. Biosynthesis of silver and gold nanoparticles using *Brevibacterium casei.* Colloids Surf B Biointerfaces **77(2),** 257-262.

Kargara H, Ghasemi F, Darroudid M. 2015. Bioorganic polymer-based synthesis of cerium oxide nanoparticles and their cell viability assays. Ceram Int **41,** 1589–1594.

Khot LR, Sankaran S, Maja JM, Ehsani R, Schuster EW. 2012. Applications of nanomaterials in agricultural production and crop protection: a review. Crop Prot **35,** 64–70.

Krishnaraj C, Jagan EG, Rajasekar S, Selvakumar P, Kalaichelvan PT, Mohan N. 2010. Synthesis of silver nanoparticles using *Acalypha indica* leaf extracts and its antibacterial activity against water borne pathogens. Colloids Surf B Biointerfaces **76,** 50–56.

Kulkarni N, Muddapur U. 2014. Biosynthesis of metal nanoparticles: A review. Journal of Nanotechnology **1-8.**

Kumar Panda M, Kumar Dhal N, Kumar M, Manjari Mishra P, Kumar Behera R. 2021. Green synthesis of silver nanoparticles and its potential effect on phytopathogens. Materials Today: Proceedings **35,** 233–238.

Ma Z, Liu J, Liu Y, Zheng X, Tang K. 2021. Green synthesis of silver nanoparticles using soluble soybean polysaccharide and their application in antibacterial coatings. International Journal of Biological Macromolecules **166,** 567–577.

Maghsoodi MR, Lajayer BA, Hatami M, Mirjalili MH. 2019. Challenges and opportunities of nanotechnology in plant-soil mediated systems: beneficial role, phytotoxicity, and phytoextraction. In: Ghorbanpour M, Wani SH (eds) Advances in Phytonanotechnology. Academic Press, Cambridge, 379-404.

Mehwish HM, Rajoka MSR, Xiong Y, Cai H, Aadil RM, Mahmood Q, He Z, Zhu Q. 2021. Green synthesis of a silver nanoparticle using *Moringa oleifera* seed and its applications for antimicrobial and sun-light mediated photocatalytic water detoxification. Journal of Environmental Chemical Engineering **9(4),** 105290.

Mortazavi SM, Khatami M, Sharifi I, Heli H, Kaykavousi K. 2017. Bacterial biosynthesis of gold nanoparticles using *Salmonella enterica* subsp. *enterica* serovar Typhi isolated from blood and stool specimens of patients. J Clust Sci **28(5),** 2997-3007.

Nahar KN, Rahaman MH, Khan GMA, Islam MK, Al-Reza SM. 2021. Green synthesis of silver nanoparticles from *Citrus sinensis* peel extract and its antibacterial potential. Asian Journal of Green Chemistry **5(1),** 135–150.

Naseer M, Ramadan R, Xing J, Samak NA. 2021. Facile green synthesis of copper oxide nanoparticles for the eradication of multidrug resistant *Klebsiella pneumonia* and *Helicobacter pylori* biofilms. International Biodeterioration & Biodegradation **159,** 105201.

Nidhi P, Agrawal S. 2021. Green Synthesis of Silver Nanoparticles Using *Ocimum tenuiflorum* Leaf Extract and its Antimicrobial Activity against Certain Pathogens. International Journal of Pharma and Bio Sciences **11(1),** 148–154.

Rai M, Yadav A, Gade A. 2009. Silver nanoparticles as a new generation of antimicrobials. Biotechnology Advances **27(1),** 76-83.

Riaz T, Mughal P, Shahzadi T, Shahid S, Abbasi MA. 2020. Green synthesis of silver nickel bimetallic nanoparticles using plant extract of *Salvadora persica* and evaluation of their various biological activities. Mater Res Express **6(12),** 1250.

Rickerby DG, Morrison M. 2007. Nanotechnology and the environment: A European perspective. Science and Technology of Advanced Materials **8(1-2),** 19–24.

Saada NS, Abdel-Maksoud G, Abd El-Aziz MS, Youssef AM. 2021. Green synthesis of silver nanoparticles, characterization, and use for sustainable preservation of historical parchment against microbial biodegradation. Biocatalysis and Agricultural Biotechnology **32,** 101948.

Salem SS, Fouda A. 2021. Green synthesis of metallic nanoparticles and their prospective biotechnological applications: an overview. Biol Trace Elem Res **199(1),** 344-370.

Shankar SS, Rai A, Ahmad A, Sastry M. 2004. Rapid synthesis of Au, Ag, and bimetallic Au core–Ag shell nanoparticles using Neem (*Azadirachta indica*) leaf broth. J Colloid Interface Sci **275(2),** 496-502.

Sharma G, Kumar A, Sharma S, Naushad M, Dwivedi RP. 2019. Novel development of nanoparticles to bimetallic nanoparticles and their composites: a review. J King Saud Univ Sci **31(2),** 257-269.

Sharma VK, Yngard RA, Lin Y. 2009. Green synthesis of silver nanoparticles and their antimicrobial activities. Advances in Colloid and Interface Science **145,** 83-96.

Singh J, Dutta T, Kim KH, Rawat M, Samddar P, Kumar P. 2018. Green synthesis of metals and their oxide nanoparticles: applications for environmental remediation. Journal of Nanobiotechnology **16(84),** 1-24.

Singh M, Srivastava M, Kumar A, Pandey KD. 2019. Biosynthesis of nanoparticles and applications in agriculture. In: Kumar A, Singh AK, Choudhary KK (eds) Role of Plant Growth Promoting Microorganisms in Sustainable Agriculture and Nanotechnology. Woodhead Publishing, Sawston. 199-217.

Sujitha MV, Kannan S. 2013. Green synthesis of gold nanoparticles using Citrus fruits (*Citrus limon, Citrus reticulata* and *Citrus sinensis*) aqueous extract and its characterization. Spectrochimica Acta Part A: Molecular and Biomolecular Spectroscopy **102,** 15–23.

Tran QH, Nguyen VQ, Le AT. 2013. Silver nanoparticles: synthesis, properties, toxicology, applications and perspectives. Adv. Nat. Sci. Nanosci. Nanotechnol **4,** 033001.

Wang G, Zhao K, Gao C, Wang J, Mei Y, Zheng X, Zhu P. 2021. Green synthesis of copper nanoparticles using green coffee bean and their applications for efficient reduction of organic dyes. Journal of Environmental Chemical Engineering **9(4),** 105331.

Yoon KY, Hoon Byeon J, Park JH, Hwang J. 2007. Susceptibility constants of *Escherichia coli* and *Bacillus subtilis* to silver and copper nanoparticles. Sci. Total Environ **373,** 572–575.